Letter

Waveguide Absorption Spectroscopy of Bovine Serum Albumin in the Mid-Infrared Fingerprint Region

Vinita Mittal, Milos Nedeljkovic, Lewis Carpenter, Ali Khokhar, Harold Chong, Goran Mashanovich, Philip N. Bartlett, and James Wilkinson

ACS Sens., **Just Accepted Manuscript** • DOI: 10.1021/acssensors.9b00215 • Publication Date (Web): 02 Jul 2019

Waveguide Absorption Spectroscopy of Bovine Serum Albumin in the Mid-Infrared Fingerprint Region

Vinita Mittal*, Milos Nedeljkovic, Lewis G. Carpenter, Ali Z. Khokhar, Harold M. H. Chong[‡], Goran Z. Mashanovich, Philip N. Bartlett[*] and James S. Wilkinson

Optoelectronics Research Centre, University of Southampton, Southampton, SO17 1BJ United Kingdom

[‡] School of Electronics and Computer Science, University of Southampton, Southampton, SO17 1BJ United Kingdom

[*] School of Chemistry, University of Southampton, Southampton, SO17 1BJ United Kingdom

ABSTRACT: Protein sensing in biological fluids provides important information to diagnose many clinically relevant diseases. Mid-infrared (MIR) absorption spectroscopy of Bovine Serum Albumin (BSA) is experimentally demonstrated on a germanium on silicon (GOS) waveguide in the 1900-1000 cm-1 (5.3-10.0 μm) region of the MIR. GOS waveguides were shown to guide light up to a wavelength of 12.9 μm. The waveguide absorption spectrum of water, showing molecular bending vibrations, was obtained experimentally and compared with a theoretical model showing good agreement. Measurement of a concentration series of BSA protein in phosphate buffered saline (PBS) from 0.1 mg/ml to 100mg/ml was performed on the waveguide using filter paper as a flow strip and the amide I, II and III peaks were observed and quantified. **Key words:** mid-infrared, waveguide, germanium, absorption spectroscopy, protein, amide

Mid-infrared (MIR) absorption spectroscopy is widely used for qualitative and quantitative analysis of biochemical species. The MIR wavelength region corresponds to wavenumbers between 4000 cm^{-1} and 400 cm^{-1} (wavelengths between 2.5 μm and 25 μm), where fundamental vibrations of molecules take place. These MIR absorptions are much stronger than those due to overtones or combinations of fundamental vibrations and rotation modes which occur in the near-infrared region (NIR) which corresponds to wavenumbers between 12500 and 4000 cm^{-1} (wavelengths 800 nm to 2.5 μm). MIR absorption features are orders of magnitude stronger than those in the NIR and provide unique absorption 'fingerprint' spectra resulting from each IR active vibration of a molecule, providing inherent molecular selectivity. The MIR absorption in proteins predominantly occurs due to vibrations of the polypeptide backbones also referred as amide bands. The most important amide bands are the amide A band between 3450-3650 cm^{-1}, associated with NH stretching vibrations, the amide I band between 1600-1700 cm^{-1}, resulting from C=O stretching, the amide II band between 1500-1600 cm^{-1}, due to CN stretching and NH in plane bending and the amide III band between 1300-1400 cm^{-1}, related to CN stretching, NH bending and CO in plane bending [1, 2]. While all proteins contain these bonds, the secondary structure or conformation of the protein, which controls protein function, results in differences in the line-shapes due to shifts in the vibrational frequencies due to changes in the hydrogen bonding environment. MIR spectroscopy is increasingly used for the analysis of secondary structure of proteins to identify biomarkers for early diagnosis of neurodegenerative diseases and cancer. The amide I band is the most investigated as its peak shape is sensitive to this secondary structure, the absorption is strong and it is not influenced by the protein side chains [2]. The amide III band is more weakly absorbing but is in a region of lower water absorption, making it attractive for measurements in aqueous media, and its line-shape is more sensitive to secondary structure, raising its potential for structural studies [3]. Analysis of the line-shape of the amide bands requires extraction of multiple overlapping spectral features, corresponding to different types of secondary structure, using double-derivative, fitting and deconvolution techniques, placing a premium on high-resolution, low noise spectra. Proteins have been studied extensively using Fourier transform infrared spectroscopy (FTIR) [4] with globar light sources. Using deuterated solutions and sample filtration, dilute protein solutions (0.2 mg/ml) were characterized with a CaF_2 flow cell of path length 55 μm [5]. However, absorption spectroscopy in aqueous solution is attractive for rapid detection of proteins in their normal environment with little sample preparation. Recently, quantum-cascade lasers (QCLs) emitting in the MIR have been used for protein spectroscopy in aqueous media with a 38 μm long flow cell made of calcium fluoride and shown to yield improved signal-to-noise ratio (SNR) with appropriate noise-reduction measures [1]. This is principally due to the higher power spectral density and brightness of QCLs, allowing longer measurement path-lengths in the presence of an absorbing aqueous background. Attenuated total reflection spectroscopy has been employed with conventional FTIR instruments, bringing the advantages of reduction in scattering for turbid media, surface-selective spectroscopy and short effective path-length without the need for narrow (10-20 μm) cuvettes or flow-channels which can cause problems with sample clogging [2]. Low-

concentration studies of aqueous solutions of proteins have been achieved

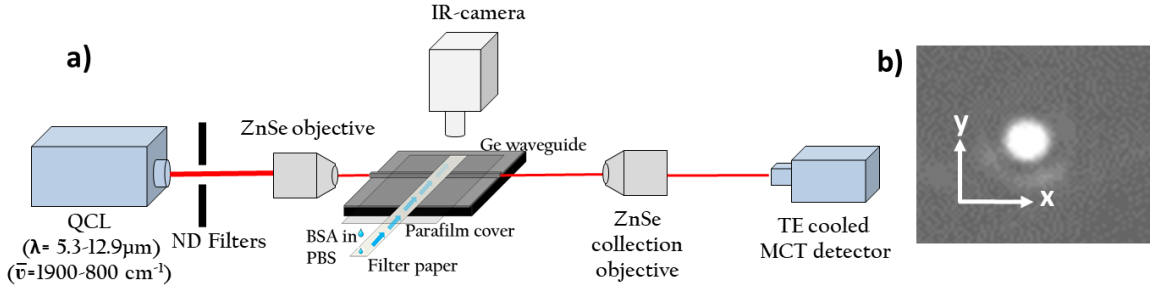

Figure 1. (a) Experimental apparatus, b) Infrared camera image of the GOS waveguide output at λ = 12.9 μm.

by combining ATR/FTIR for diagnosis and segregation of dementia [6], a calcium fluoride immuno-IR sensor was used to detect the structural changes in amide I peak [7], a new method of immobilization of proteins on Ge ATR is presented to monitor enzymatic activity using MIR spectroscopy of amide peaks [8] and a Ge ATR crystal was used to study BSA protein by electrophoresis where a voltage is applied across the sensor to enhance the accumulation of proteins on the sensor surface [9].Optical waveguide approaches to ATR spectroscopy offer (i) enhanced sensitivity over conventional ATR crystals because the effective number of "bounces" per unit length is greatly increased, (ii) improved stability and path-length selection due to the continuous field at the waveguide surface, and (iii) advantages of low-cost and multisensor integration arising from the mass manufacturing approaches of microelectronics used in waveguide fabrication. There have been a few demonstrations of waveguide spectroscopy of biochemical species, including proteins, in the MIR region. These include the use of a 14 μm thick and 500 μm wide diamond waveguide to study the secondary structure within the amide I peak of BSA at a concentration of 10 mg/ml [10].

In this work, absorption spectroscopy of Bovine Serum Albumin (BSA) in phosphate buffered saline (PBS) is demonstrated using the evanescent field of a germanium on silicon (GOS) waveguide operating between 1900-1000 cm^{-1} (5.3-10 μm) in the MIR. All three of the amide I, II and III peaks are observed for the first time on a waveguide platform. In order to introduce the liquid analyte into the waveguide evanescent field, a simple flow-strip using filter paper was used. It has been established that the presence of filter paper on the surface of waveguide does not itself significantly alter the optical transmission of the waveguide [11]. Paper-based fluidics is widely used for biochemical assays and its integration with waveguide evanescent spectroscopy offers the potential for improved quantification.

Measurements were carried out using the apparatus shown in Fig.1 a). A quantum cascade laser system (QCL) (Block Engineering Inc.) tunable from 1900-800 cm^{-1} that has four coupled chips, was used as a source, and two zinc selenide (ZnSe) objective lenses were used for input and output coupling to the waveguides. A thermoelectrically (TE) cooled mercury cadmium telluride (MCT) detector (VIGO System) was used to collect the signal from the ZnSe collection objective. The signal from the MCT detector was recorded on a computer which also controlled the QCL wavelength scans, and a software package (LaserTune), was used to process the spectra.

Straight 3 μm thick and 20 μm wide GOS were used. Six inch GOS wafers were bought commercially from IQE Silicon Compounds Ltd. The fully etched channel waveguides were fabricated using lithography and ICP etching with fluorine chemistry. Waveguide facets of optical quality were prepared using a dicing saw [12]. The GOS waveguides used in this work were designed using COMSOL to ensure guidance at wavelengths up to λ = 12.9 μm. The theoretical spot sizes for the fundamental TM mode were found to be 10.62 μm in the width (x) direction and 2.7 μm in the depth (y) direction. At this wavelength the waveguides were predicted to be monomode in the y direction but multimode in the x direction. Simulations of mode profiles of GOS waveguides in water were not significantly different in shape than when in air due to the high refractive index contrast between Ge and air/water.

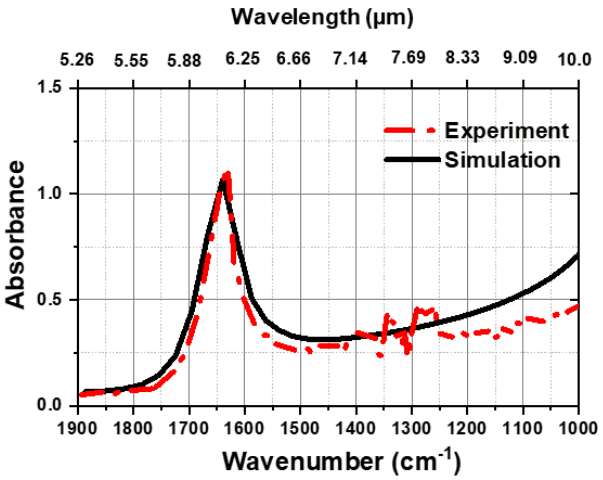

Figure 2. Experimental and simulated waveguide absorption spectra of water of 3.5 mm path-length.

The QCL was tuned to a wavelength of 12.9 μm and its output was launched into the waveguide in TM polarisation. The waveguide output was imaged using an infrared camera (Xenics-Gobi 640) placed after the output objective lens and is shown in Fig. 1 b). The QCL was then tuned across the full wavelength range down to 5.3 μm and the waveguide output was clearly visible across the full range, showing that these waveguides guided continuously from 5.3 μm to 12.9 μm. In

order to confirm the calibration of the system for absorbance and wavenumber, the MIR absorption spectrum of deionized (DI) water was measured on the waveguide and compared with the published spectra. In order to introduce the analyte into the waveguide evanescent field and to define the pathlength of the analyte, a 180 μm thick strip of filter paper (Fisher) 3.5 mm wide and 4 cm long was placed on the waveguide and a cover of parafilm about 5-6 mm wide was placed over it to reduce evaporation, as shown in Fig. 1 a).

The output power spectrum of the waveguide with filter paper and parafilm alone was first recorded as a reference spectrum, by sweeping the QCL frequency between 1000 cm^{-1} and 1900 cm^{-1} to include the regions of water and amide band absorption and recording the waveguide output power using the MCT detector. Drops of DI water were then pipetted onto the exposed tail of the filter paper and allowed to travel to the waveguide. The waveguide output power spectrum in the presence of DI water (sample spectrum) was then recorded. The absorption due to the presence of water was deduced by dividing the sample spectrum by the reference spectrum, and the resultant DI water absorption spectrum is plotted in Fig 2. The frequency resolution of all scans was 1 cm^{-1} and their duration was 10 s. The COMSOL model used for the mode field distributions was used to determine the complex modal effetive index of the fundamental mode vs wavelength and hence the theoretical waveguide absorption spectrum, which is also shown in Fig 2. The model takes into account the published optical constants of water [13]. The broad absorption peak of water which is due to H-O-H bending vibrations is observed at 1635 cm^{-1}. The simulated and experimental graphs plotted in Fig. 2, which have not been normalized, show good agreement, confirming the wavenumber and absorbance calibration. However, the experimental graph deviates slightly from theory for wavenumbers above 1400 cm^{-1} due to the noise of the system and low scattering losses of the waveguides at longer wavelengths. The discontinuity in experimental data around 1300 cm^{-1} is due to the low laser power and the switching from one QCL chip to another.

BSA was used to demonstrate waveguide protein spectroscopy. A phosphate buffer solution (PBS) of 0.01 M concentration with pH 7.0 was used to prepare the protein solutions. A stock solution of 10% BSA with concentration 100 mg/ml (Sigma Aldrich) was obtained and solutions of lower concentration were made from this by diluting it in PBS solution of the same molarity. Solutions with concentration ranging from 0.1 mg/ml to 100 mg/ml were prepared. For the waveguide measurements, a filter paper strip 3 mm wide and 4 cm long was placed on the waveguide and a transmission spectrum with PBS alone was recorded as a reference spectrum. The waveguide surface was cleaned and a solution of 10 mg/ml was pipetted on a fresh filter paper strip on the waveguide. The parafilm cover was not used here and the BSA solution was left to evaporate. The waveguide output power spectrum was then recorded at 1 to 2 minute intervals. The frequency resolution of all scans was 1cm^{-1} and had a duration of 10 s. To calculate the absorption due to protein alone, the transmitted power spectra from the BSA sample were divided by the transmitted power spectrum from the pure PBS reference. The resultant BSA absorption spectrum with respect to time is shown in Fig. 3, showing increasing absorption with time mainly due to water evaporation. The obtained spectra were smoothed by performing adjacent averaging of 10 data points around each data point in the data and replacing that point with a new filtered point. The original unprocessed data is shown in the Supplement as Figure S1. The BSA absorption spectra in Fig. 3 show all the three amide I, II and III peaks at 1645, 1545 cm^{-1} and between 1200-1350 cm^{-1} respectively. While evaporation will not be used in normal operation of this sensor for protein quantification, these data allow observation of amidepeak positions and the ratio between amide I, II and III peaks as a function of concentration without changing any other parameters. The spectra are in good agreement with the literature suggesting that the BSA does not denature or significantly change secondary structure at the waveguide surface [5, 9, 14]. The absorption spectra in Fig. 3 also shows the CH bending absorption peak at 1455 cm^{-1}, COO^- symmetric stretching peak at 1402 cm^{-1} and in-plane CH bending absorption between 1000 and 1100 cm^{-1} [15].

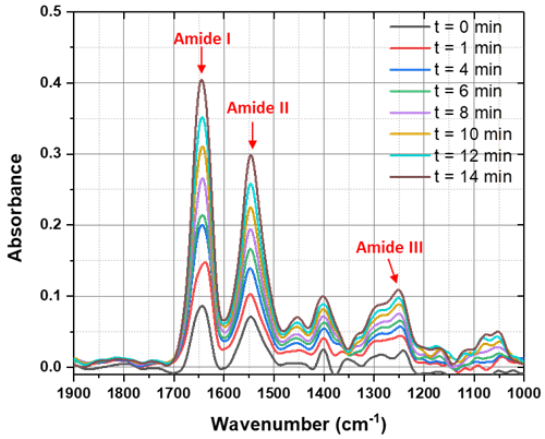

Figure 3. Waveguide absorbance of 10 mg/ml BSA in PBS solution with respect to time

To determine the concentration dependence of the waveguide absorption measurements, a dilution series of BSA in PBS was performed with concentrations of 0, 0.1, 1, 10, 25, 50 and 100 mg/ml. In order to avoid the evaporation observed in Figure 3, parafilm was again used to cover the filter paper as shown in Figure 1(a). For each concentration a fresh filter paper with parafilm over-layer was used and Figure 4 (a) shows the protein absorption spectrum (referenced to PBS) for each concentration of BSA. The graph shows a systematic increase in the three amide peak heights with increasing concentration of BSA, as expected. The peak absorption for the amide I and II band at a wavenumber of 1645 cm^{-1} was plotted versus concentration of BSA and is shown in Figure 4 (b) and S2 respectively. The error bars were estimated from the standard deviation of six measurements at 1880 cm^{-1}, away from the BSA absorption absorption and we believe these errors to be dominated by input coupling and laser fluctuations. The absorbance for 10 mg/ml BSA concentration was compared with the absorbance for 10 mg/ml BSA plotted in Fig. 3 for t = 0 min and was found to be consistent.

This is the first reported measurement of all three amide peaks I, II and III on a thin film waveguide and the first systematic study of waveguide absorption spectroscopy of a

dilution series of BSA in PBS. Absorption spectra have been obtained for a concentration of 0.1 mg/ml and more dilute solutions will be accessible with improvements in stability and SNR engineering. The strong absorption of water over the entire MIR region and an overlapping OH and the Amide I peak in the region of

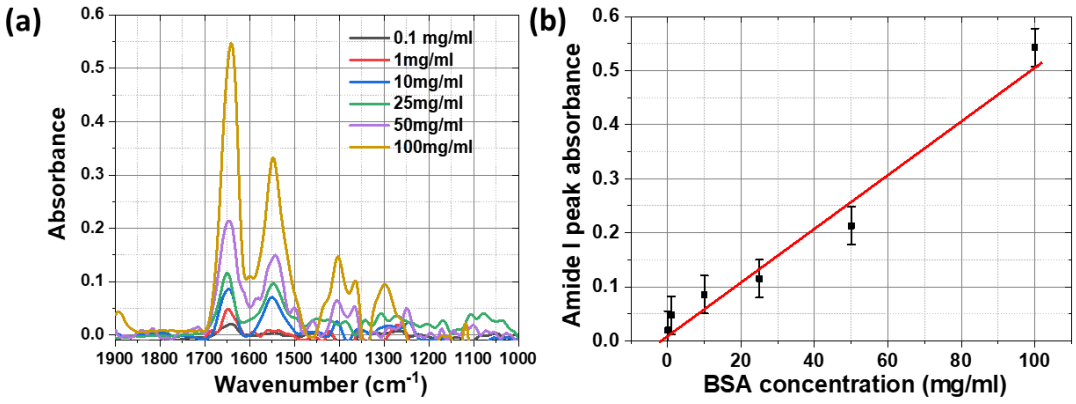

Figure 4. (a) Waveguide absorption spectra of BSA in PBS at different concentration and (b) Amide I peak height with respect to BSA concentration, for a waveguide path-length of 3 mm.

1600-1700 cm^{-1} severely limits the useable path-length in any MIR approach and hence the sensitivity to protein absorption, but the combination of QCL sources and optical waveguides allows high signal, precise optimization of the path-length, and avoids the problems of turbid media and the need for narrow cells which clog easily. Waveguides can provide a precisely controlled interaction length to match the absorption of a specific analyte and this could be maximized in a small on-chip footprint by introducing engineered bends and spirals [16]. The waveguide approach has all the advantages of conventional ATR techniques, being particularly well-suited to studies of interactions in monolayers at surfaces but with the added benefits of lower cost, more compact design and potential integration of reference channels, for example. In the present work, 3 µm thick GOS waveguides have been used, but the sensitivity and detection limit can be tailored according to the wavelength range of interest by using waveguides of different thickness.

The demonstration of present work that combines thin film waveguides and QCL operating in the MIR finger print region allows new possibilities of sensing important biomolecules for point of care diagnostics by utilizing high selectivity of MIR signatures.

Corresponding Author

v.mittal@soton.ac.uk

Supporting Information

The following files are available free of charge.
S1: Waveguide absorbance of 10 mg/ml BSA in PBS solution with respect to time, without smoothening the peaks.
S2: Amide II peak height with respect to BSA concentration.

Data supporting this Letter are openly available from the University of Southampton repository at https://doi.org/10.5258/SOTON/D0940

ACKNOWLEDGMENTS

VM and JSW thank the European Union (ERC) (FP7/2007-2013, 291216) for support; MN thanks the Royal Academy of Engineering for their support (RF201617/16/33); VM, AZK, HMHC and GM acknowledge the EPSRC Platform grant (EP/N013247/1) and High Value Photonic Manufacturing (EP/N00762X/1); PNB thanks the Royal Society for a Wolfson Research Merit Award.

REFERENCES

(1) Alcaráz, M. R.; Schwaighofer, A.; Kristament, C.; Ramer, G.; Brandstetter, M.; Goicoechea, H.; Lendl, B. External-cavity quantum cascade laser spectroscopy for mid-IR transmission measurements of proteins in aqueous solution. Anal. Chem. **2015**, 87, 6980-6987.

(2) López-Lorente, Á. I.; Mizaikoff, B. Mid-infrared spectroscopy for protein analysis: potential and challenges. Anal. Bioanal. Chem. **2016**, 408, 2875-2889.

(3) Cai, S.; Singh B.R. A distinct utility of the amide III infrared band for secondary structure estimation of aqueous protein solutions using partial least squares methods. Biochemistry. **2004**, 43, 2541-2549.

(4) Barth A. Infrared spectroscopy of proteins. Biochim. Biophys. Act. **2007**, 1767, 1073-1101.

(5) Baldassarre, M.; Barth, A. Pushing the detection limit of infrared spectroscopy for structural analysis of dilute protein samples. Analyst. **2014**, 139, 5393-5399.

(6) Paraskevaidi, M.; Morais, C.L.; Lima, K.M.; Snowden, J.S.; Saxon, J.A.; Richardson, A.M.; Jones, M.; Mann, D.M.; Allsop, D.; Martin-Hirsch; P.L. and Martin. F.L. Differential diagnosis of Alzheimer's disease using spectrochemical analysis of blood. Proceedings of the National Academy of Sciences, **2017**, 114, E7929-E7938.

(7) Von Bergen, M.; Barghorn, S.; Biernat, J.; Mandelkow, E.M.; Mandelkow, E. Tau aggregation is driven by a transition from random coil to beta sheet structure. Biochimica et Biophysica Acta (BBA)-Molecular Basis of Disease **2005**, 1739, 158-166.

(8) Schartner, J.; Güldenhaupt, J.; Gaßmeyer, S.K.; Rosga, K.; Kourist, R.; Gerwert, K.; Kötting, C. Highly stable protein immobilization via maleimido-thiol chemistry to monitor enzymatic activity. **2018**., Analyst, **143**, 2276-2284.

(9)Yang, Z.; Fah, M.K.; Reynolds, K.A.; Sexton, J.D.; Riley, M.R.; Anne, M.L.; Bureau, B.; Lucas, P. Opto-electrophoretic detection of bio-molecules using conducting chalcogenide glass sensors. Opt. Express. **2010**, 18, 26754-26759.

(10) López-Lorente, Á.I.; Wang, P.; Sieger, M.; Vargas Catalan, E.; Karlsson, M.; Nikolajeff, F.; Österlund, L.; Mizaikoff, B. Mid-infrared thin-film diamond waveguides combined with tunable quantum

cascade lasers for analyzing the secondary structure of proteins. Phys. Status Solidi A. **2016,** 213, 2117-2123.

(11) Mittal, V.; Nedeljkovic, M.; Rowe, D.J.; Murugan, G.S.; Wilkinson, J.S. Chalcogenide glass waveguides with paper-based fluidics for mid-infrared absorption spectroscopy. Opt. Lett. **2018**, 43, 2913-2916.

(12) Mittal, V.; Aghajani, A.; Carpenter, L.G.; Gates, J.C.; Butement, J.; Smith, P.G.; Wilkinson, J.S.; Murugan, G.S. Fabrication and characterization of high-contrast mid-infrared $GeTe_4$ channel waveguides. Opt. Lett. **2015** 40, 2016-2019.

(13) Hale, G.M.; Querry, M.R. Optical constants of water in the 200-nm to 200-μm wavelength region. Appl. Opt. 1973, 12, 555-563.

(14) Infrared Spectroscopy: Fundamentals and Applications by Barbara Atuart, John Wiley & Sons Ltd., United States, **2004**.

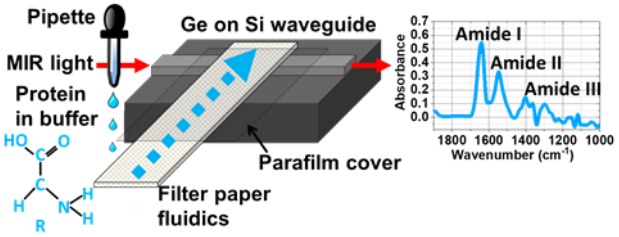

(15) Infrared Spectral Interpretation by Brian Smith, CRC Press, United States, **1999**.

(16) Li, W., Anantha, P., Lee, K.H., Qiu, H.D., Guo, X., Goh, S.C.K., Zhang, L., Wang, H., Soref, R.A. and Tan, C.S. Spiral Waveguides on Germanium-on-Silicon Nitride Platform for Mid-IR Sensing Applications. IEEE Photonics Journal, **2018**, 10, 1-7.

For TOC only